



Surface charge compensation for a highly charged ion emission microscope

J.W. McDonald^{a,*}, A.V. Hamza^a, M.W. Newman^a, J.P. Holder^a,
D.H.G. Schneider^a, T. Schenkel^b

^aLawrence Livermore National Laboratory, L 472, Livermore, California 94550, USA

^bE.O. Lawrence Berkeley National Laboratory, USA

Received 13 November 2003; received in revised form 25 May 2004; accepted 14 June 2004

Abstract

A surface charge compensation electron flood gun has been added to the Lawrence Livermore National Laboratory (LLNL) highly charged ion (HCI) emission microscope. HCI surface interaction results in a significant charge residue being left on the surface of insulators and semiconductors. This residual charge causes undesirable aberrations in the microscope images and a reduction of the time-of-flight (T-O-F) mass resolution when studying the surfaces of insulators and semiconductors. The benefits and problems associated with HCI microscopy and recent results of the electron flood gun-enhanced HCI microscope are discussed.

© 2004 Elsevier B.V. All rights reserved.

PACS: 82.80.Rt; 41.75.Ak; 39.10.+j

Keywords: Highly charged ion T-O-F SIMS; Surface analysis; Charge compensation

1. Introduction

In the last few years increasing demands of the semiconductor industry for materials characterization at high-spatial resolution have driven the instrument development field. To meet the increasing demands of the semiconductor industry for materials characterization at very high-spatial

resolution an impressive array of instruments have been developed (transmission electron microscopy, scanning-tunneling electron microscopy, etc.). There is an equally impressive array of instruments and techniques available to determine material composition (secondary ion mass spectroscopy, Auger electron spectroscopy, photoelectron spectroscopy, etc.). The Lawrence Livermore National Laboratories (LLNL) highly charged ion (HCI) driven emission microscope has the potential to provide both high-spatial resolution and very sensitive

*Corresponding author.

E-mail address: mcdonald6@llnl.gov (J.W. McDonald).

compositional analysis simultaneously and has been described in detail by Hamza et al. [1]. Emission microscopes are a special class of electron microscopes that accelerate and image low energy electrons and other charged particles from a planar surface. The history of emission microscopes began more than 100 years ago (see Ref. [2]). The HCI emission microscope described here is a combination of two emission microscopes developed in the 1960s. The first, an Ar^+ ion beam-induced electron emission microscope [3] where the kinetic emission of electrons forms an image. The second, a secondary ion emission microscope [4] where an ion beam is used to sputter secondary ions, which are imaged. In the present instrument, electrons and secondary ions are imaged and the mass of the secondary ions is determined by time-of-flight (T-O-F). Thus, a variety of contrast imaging modes are available.

The emission microscope described here uses HCIs as the excitation source. The highly charged ions bring four crucial advantages, a large secondary electron yield, high secondary ion yields, high ionization probability of the secondary emission, and high molecular yields.

Highly charged ions carry considerable potential energy (the sum of the ionization potentials of the highly charged ion) to surfaces and this energy is released in the first few femtoseconds of surface interaction resulting in a highly localized energy deposition in the first few atomic layers of the surface [5]. In contrast is the case of singly charged ion-induced secondary ion mass spectroscopy (SIMS) where most of the energy transferred to the surface comes from the kinetic energy of the projectile ion. This kinetic transfer is a multistep, relatively low cross-section process that is distributed across a comparatively deep collision and is not localized to the surface layers. The localized energy deposition from a HCI/surface interaction results in very high (100s of electrons per primary ion) electron [6,7] and (greater than one) secondary ion yields [8]. The ratio of the secondary ion yield to the secondary neutral yield gives ionization probabilities of 10% for HCI excitation [9]. This very high-electron yield is employed to produce the very high-spatial resolution. Present photoelectron emission microscopes can achieve

less than 10 nm resolution imaging single electron events [10]. The high secondary ion yield, particularly the high secondary molecular ion yield, and the high ionization probability that HCI excitation produces offer the potential of providing highly sensitive compositional information at high-spatial resolution.

Unfortunately, the potential energy associated with the HCI surface interaction also involves charge deposition. This charge is of little consequence when the HCI is interacting with a conductor where the high electron mobility can dissipate the charge. However, in the case of semiconductors and insulators the surface charges up. This surface charging leads to serious distortions in the images produced in the HCI emission microscope as well as a significant reduction in the resolution of the secondary ion mass T-O-F spectra. While charge neutralization of the sort described here is well known in conventional SIMS, this paper describes its application to a HCI SIMS microscope.

2. Experiment

In this microscope, a beam of highly charged ions in a single-charge state (i.e. Xe^{44+}) from the LLNL electron beam ion trap (EBIT) [11] is focused onto the sample to be analyzed. The secondary electrons or ions are accelerated and focused onto a channel plate detector with a resistive anode position sensitive imaging system. The experimental setup is described in detail by Hamza in Ref. [1]. The main disadvantage of employing HCIs as the excitation source is the charge built up on the surface of the sample when studying semiconductors and insulators. In an effort to neutralize the charge left on the surface we have installed an electron flood gun. The electron flood gun, shown schematically in Fig. 1 (left) was put together from parts on hand in our laboratory. The timing of the electron flood gun emission, sample bias, HCIs, and data acquisition were controlled by a timing sequencer. The filament current, cathode bias and duty cycle between the HCI and electron exposure were

varied to determine the optimum operating conditions for each sample and effective ion current.

The secondary ion/electron imaging lensing system was designed with six radial ports providing line-of-sight access to the target surface. The secondary ions/electrons are collected from the center of the sample and imaged through the magnification optics onto the position sensitive detector. At present three of the access ports are used; one for the primary ion excitation, one for the UV excitation, and one for the electron flood gun neutralization. The physical layout of the target interaction region is shown from the view point of the position sensitive detector in Fig. 1 (right).

The EBIT source can deliver 10^6 primary ions per second to the target however the data collection rate was limited to 1000 secondaries per second due to limitations of the available T-O-F timing electronics. The data for the resulting images was collected over a period of approximately 1–3 h each.

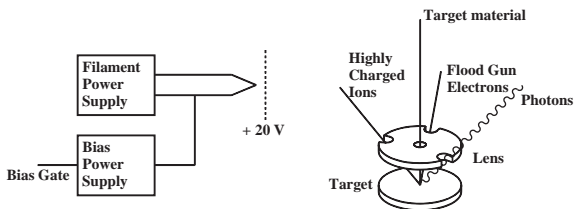


Fig. 1. Schematic diagram and Layout of Sample Access.

3. Results

To demonstrate the operation of the electron flood gun we have imaged an L-shaped scratch on a glass microscope slide. This microscope slide was cleaned with alcohol and the scratch was made with a diamond scribe. The image on the left of Fig. 2 is of the apex of the L at a magnification of $40\times$ (field of view is $950\mu\text{m}$) and the image on the right is near the apex of the L at a magnification of $\approx 90\times$ (field of view is $400\mu\text{m}$). The images obtained with out the flood gun compensation on showed no contrast from the scratch. Secondary ion T-O-F spectra were collected from both the undamaged and damaged areas of the sample. The undamaged areas of the sample showed higher ratios of $\text{C}_2\text{H}_{x=0-2}$ to SiO_x as would be expected from areas where the surface hydrocarbons have not been removed. T-O-F spectra showing negative ions from the undamaged and damaged areas of the sample are shown in Fig. 3. To demonstrate an interesting feature of this analysis process, we point out that there is no boron present in the T-O-F spectra indicating that the microscope slide we employed in this test was not Pyrex/BoroSilicate glass.

As a second demonstration of the effectiveness of the electron flood gun we imaged the surface of a pressed powder of a high explosive (poor electrical conductor). Initial imaging tests on this bare surface proved unusable due to surface charging. A first attempt to improve the image and T-O-F SIMS spectra was to press an $18\mu\text{m}$

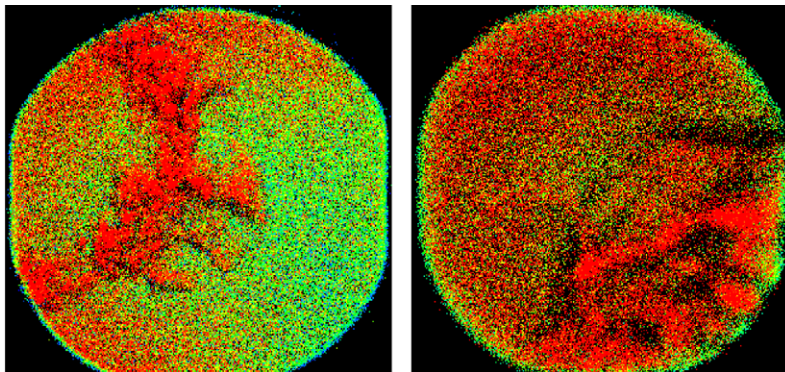


Fig. 2. Left side apex of L scratch on microscope slide at $40\times$, right side near apex of scratch at magnification of $90\times$.

(spacing) nickel grid into the surface to dissipate the charge buildup. The image on the left side of Fig. 4 shows an image of the high explosive with the grid pressed into the surface. The metal grid can clearly be seen as areas of high electron emission (red), an area of positive charge caused at the center of the grid and apparent area of high electron emission. This apparent area of high emission is due to a focusing effect of the positively-charged surface. The right side of Fig. 4 shows the same target with the electron flood gun turned on. The charged induced focusing effect is has been eliminated greatly improving the image

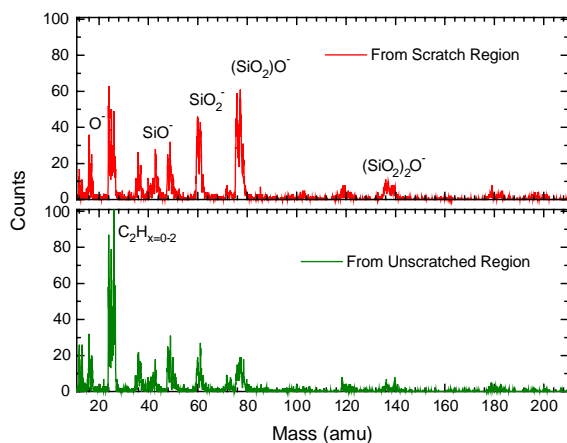


Fig. 3. Glass slide T-O-F spectra, top from scratched region, bottom from unscratched region. Note the higher ratios of $C_2H_{x=0-2}$ to SiO_x from the unscratched region.

resolution. T-O-F spectra from the same surface is shown in Fig. 5 where the top is without charge compensation and the bottom is with charge compensation. The improvement in the resolution of the T-O-F spectrum is apparent. The water peak is well defined and the C_2 , C_2H , and C_2H_2 series of peaks are clearly distinct.

By biasing the sample positively we were able to collect and image positive secondary ions from the sample. A positive ion image from the end of scratch on the microscope slide, with a magnification of 40x (field of view is $950\ \mu\text{m}$) is shown in Fig. 6. As with the negative ion image the positive

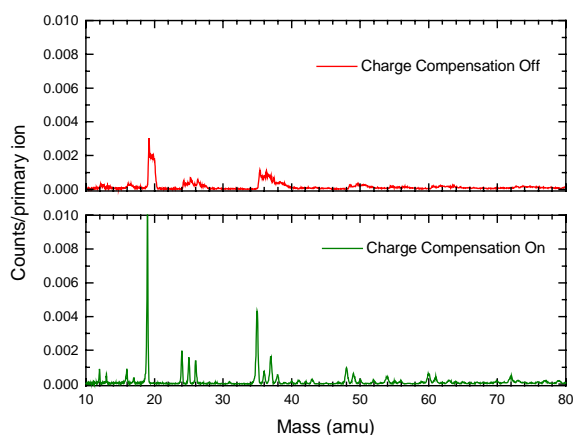


Fig. 5. Charge compensation effects on T-O-F spectrum of high explosive (insulating matrix) with $18\ \mu\text{m}$ metallic grid pressed into the surface.

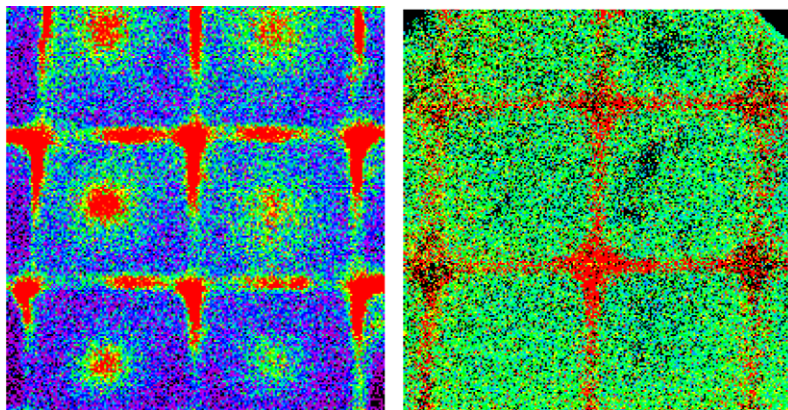


Fig. 4. High explosive matrix with a $18\ \mu\text{m}$ nickel grid pressed onto the front surface, with a charge compensation (right side), without on the left side.

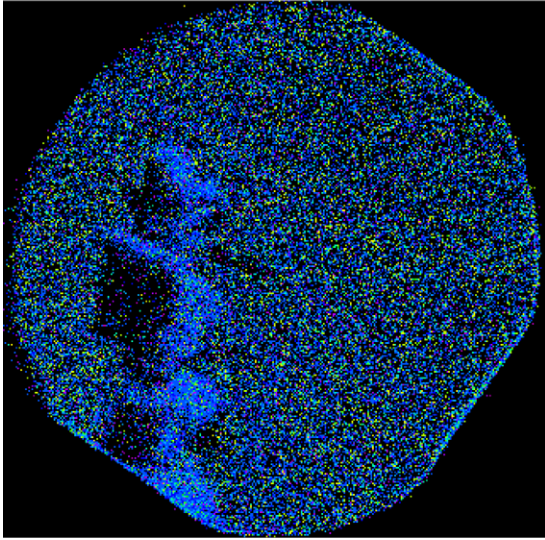


Fig. 6. Positive ion image of the end of the I scratch at $40\times$, field of view is $950\ \mu\text{m}$.

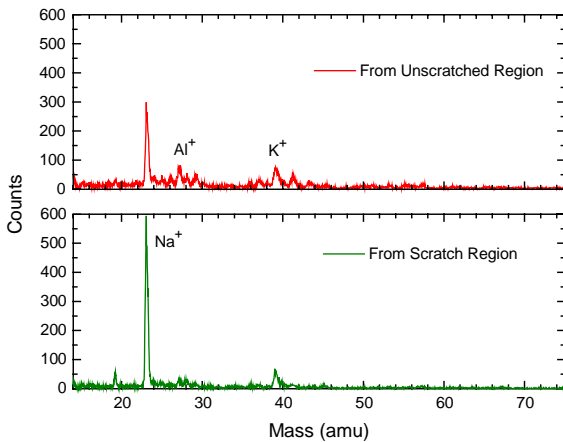


Fig. 7. Positive ion T-O-F- spectra from microscope slide. Top unscratched region, bottom scratched region. Note the increase in sodium and the decrease in aluminum from the scratched region.

images with out charge compensation show no contrast. Fig. 7 shows a positive ion T-O-F- spectra from the same microscope slide. The top

spectrum is from the unscratched region, and the bottom spectrum is from the scratched region. Note the increase in sodium and the decrease in aluminum from the scratched region.

While the spatial resolution of this unique device could be improved, the addition of electron flood gun charge compensation, has greatly extended the utility of this HCI T-O-F microscope by allowing the analysis and imaging of insulators and semiconductors.

Acknowledgments

This work was performed under the auspices of the US Department of Energy by University of California Lawrence Livermore National Laboratory under Contract No. W-7405-ENG-48.

References

- [1] A.V. Hamza, A.V. Barnes, E. Magee, M. Newman, T. Schenkel, J.W. McDonald, D.H. Schneider, *Rev. Sci. Instrum* 71 (2000) 2077.
- [2] O.H. Griffith, W. Engel, *Ultramicroscopy* 36 (1991) 1.
- [3] H. Düker, *Z. Metallkd.* 51 (1960) 314.
- [4] R. Castiang, G. Slodzian, *Proceedings of the European Regional Conference on Electron Microscopy (Nederlandse Vereniging voor Electron Microscopie)*, Delft, vol. 1, 1960, p. 169.
- [5] T. Schenkel, M.A. Briere, H. Schmidt-Böcking, K. Bethge, D.H. Schneider, *Phys. Rev. Lett.* 78 (1997) 2481.
- [6] J. McDonald, D. Schneider, M. Clark, D. DeWitt, *Phys. Rev. Lett.* 46 (1992) 2297.
- [7] F. Aumayr, H. Kurz, D. Schneider, M. Briere, J.W. McDonald, C.E. Cunningham, H.P. Winter, *Phys. Rev. Lett.* 71 (1993) 1943.
- [8] T. Schenkel, A.V. Barnes, M.A. Briere, A. Hamza, A. Schach von Wittenau, D. Schneider, *Nucl. Instrum. Methods Phys. Res. B* 125 (1997) 153.
- [9] T. Schenkel, A.V. Barnes, A.V. Hamza, D.H. Schneider, J.C. Banks, B.L. Doyle, *Phys. Rev. Lett.* 80 (1998) 4325.
- [10] G.F. Rempfer, O.H. Griffith, *Ultramicroscopy* 47 (1992) 35.
- [11] D. Schneider, M.W. Clark, B.M. Penetrante, J. McDonald, D. DeWitt, N.J. Bardsley, *Phys. Rev. A* 44 (1991) 3119.